Torrefaction of Short Rotation Coppice Willow. Characterization, hydrophobicity assessment and kinetics of the process

Ana Álvarez, Sergio Migoya, Roy Menéndez, Gemma Gutiérrez, Consuelo Pizarro*, Julio L. Bueno

Department of Chemical and Environmental Engineering, Faculty of Chemistry, University of Oviedo, Julián Clavería 8,33006 Oviedo, Asturias, Spain

*corresponding author

Email address:

ABSTRACT

Short Rotation Coppice Willow (SRCW) is one of the newest sources of renewable energy. Torrefaction enhances the initial poorest characteristics of SRCW, such as hygroscopicity or low heating value compared to traditional fuels, to use it as a fuel. Non-oxidative and oxidative torrefaction of SRCW were compared. Torrefaction were conducted within the range 200-240 ºC and torrefied SRCW and released gases were characterized (proximate, ultimate, compositional and heating value analysis as well as hydrophobicity assessment, Py-GC/MS and chemical-kinetics parameters). At optimal torrefaction temperature, mass and energy yields were around 88 % and 93 %, respectively, moisture was reduced up to 1.22-1.28 % and H/C and O/C atomic ratios up to 1.4 and 0.6, respectively. Biomass turns hydrophobic since contact angle increase and the amount of water absorb decrease in contact angle and liquid penetration studies, respectively. The global reaction order was 2 and kinetic constant values were in the range 4.6 10^{-5} s^{-1} to 3.6 10^{-5} s^{-1}.

KEYWORDS: torrefaction, compositional analysis, hydrophobicity, Py-GC/MS, torrefaction kinetics

1. INTRODUCTION

Energy crops plantations are stable sources of renewable energy in the long term and consequently contribute to reduce foreign energy dependency of the countries [1,2]. Short rotation coppice biomass grows relatively fast and requires low agro-chemical inputs. One of the main stands that can be grown as a Short Rotation Coppice is the Willow (SRCW). However, SRCW exhibits the same poor properties as other biomass compared to coal, these are poor grindability, high oxygen content, low energy density, hydrophilic behaviour [3]. However, it can be upgraded by means of torrefaction and, as a result, torrefied SRCW exhibits some better properties such as higher energy content, hydrophobic behaviour or improved grindability [4], which lead to benefits in transportation, storage, handling and feeding. Dry torrefaction could be carried out under two different conditions, namely oxidative and non-oxidative torrefaction. In the first one, the carrier gas could be air, flue gas and other gases with different oxygen contents. In the latter one, the most common carrier gas is nitrogen.

A condensable fraction is produced during torrefaction, which consist of lignin and sugar derivatives among other compounds. Consequently, torrefaction can be considered as a conversion technology in multiproduct biorefineries in the same way as pyrolysis [5].

Py-GC/MS is an appropriate technique for study condensable fraction produced during torrefaction. In addition, it could be used to estimate the S/G ratio of

lignin, being Guaiacyl (G), syringyl (S) and p-hydroxyphenyl (H) units the main components of lignin.

A few studies have been conducted focusing on how the torrefaction affects the main components (lignin, cellulose and hemicellulose) of biomass and its torrefaction kinetics [6–9]. According to these results, hemicellulose is the component that most degrades in torrefaction, even at low temperatures and the reaction order of xylan was found as third order, but within torrefaction process there are multiple reactions and not only the hemicellulose fraction is involved in the process. Some studies are focused on torrefaction of willow [9–13], in which there has been a great deal of research in solid fraction analysis of torrefied biomass and torrefaction kinetics. However, most of previous works do not study Willow harvested as a short rotation coppice and in almost all cases focus only on solid characterisation and not the released gases or properly study de hydrophobicity behaviour of torrefied biomass. Besides, there are lack of explanation about how main components of biomass are affected by torrefaction in real SRCW samples. Py-GC/MS was used to study the gases released during the pyrolysis of several kinds of biomass [14–16], but it was not possible to find this analytical technique applied in torrefaction studies.

Hydrophobicity measurements are usually obtained through the equilibrium moisture content [3,17–19]. However, measurements were not found in scientific articles in which biomass undergoing torrefaction was characterized. Wettability studies usually involve the measurement of contact angles as the primary data, which indicates the degree of wetting when a solid and liquid interact [20]. Small contact angles (<90°) correspond to low hydrophobicity

(high wettability), while large contact angles (>90°) correspond to high hydrophobicity (low wettability) [21]. Surface roughness differences are responsible for many of the differences in contact angle values of the different species and different wood surfaces [22,23].

Other technique is the liquid penetration; it is based on the gained water measuring during time, while the powder packed on a cylindrical tube is in contact with the liquid surface. This technique has the masking disadvantage that liquid evaporation could take place in samples where penetration rate is slow [24].

As a general trend, samples with highly hydrophilics (contact angle lower than 90°) are recommended to be determinated by liquid penetration method buy a tensiometer, while samples with high hydrophobicity (contact angle larger than 90°) are recommended to be measured by sessile drop meter by a goniometer [25]. Even large of studies described the liquid penetration technique for wettability measurements of solids, most applications are focused on pharmaceutical and food powder [26–28] being scarce their application on biomass characterization [29]

The present study focuses on the non-oxidative and oxidative torrefaction of SRCW. The torrefied SRCW was fully characterized obtaining mass and energy yields of the torrefaction process, carrying out proximate and ultimate analyses, compositional analysis and obtaining high heating value, the hydrophobicity was assessed and optimal torrefaction temperature was found. Furthermore, isothermal kinetics of torrefaction at the optimal temperature were obtained using a thermogravimetric analyser.

2. MATERIAL AND METHODS

2.1 Sample preparation

SRCW (Salix viminalis x (S. schwerinii x S. Viminalis (clone Olof)) was collected from experimental trial established on abandoned mining land. Biomass particle size was reduced to the range 710 - 1000 µm through grinding and sieving processes and raw biomass samples were characterized (Table 1).

Table 1. Characterization of raw biomass samples.

Proximate analysis, %	
Moisture	6.90±0.05
Ash	1.24±0.01
Volatiles	75.93±0.05
Fixed carbon	15.93±0.05
Ultimate analysis, %	
C	45.31±0.02
H	6.37±0.09
S	0.13±0.01
N	0.16±0.06
O	48.03±0.09
HHV, J/g	18369±19

2.2 Torrefaction experiments

Oxidative and non-oxidative torrefaction experiments were carried out in a tube furnace reactor (Carbolite MTF 12/38/150) at five different temperatures every 10 ºC within the range of 200-240 ºC. Air was used as oxidative atmosphere, while nitrogen was selected as inert atmosphere. The torrefaction temperature was held for 20 min, this was previously selected to assure a completed torrefaction based on TGA data together with previous trials in our set-up with this sample, and the flux of oxidizing or inert gas was set to 1 L/min. At least 8

replications for each temperature were conducted. The temperature range selected is due to the nature of SRCW, since it is a poor lignified wood and consequently, its resistance towards thermal treatments under oxidative atmospheres is low.

2.3 Solid analysis

Proximate analysis and heating value were carried out according to the ASTM Standards [30–33] in a muffle furnace (Carbolite CWF 1100), three replications of each sample were carried out, while ultimate analysis was conducted using an elemental analyser (Elementar Vario Macro CHNS). In compositional analysis, lignin, holocellulose and cellulose were quantified according to NREL procedure, ASTM D1104 standard and TAPPI T212 standard, respectively [34–36], three replications of each sample were carried out. Scanning Electron Microscope (MEB JEOL-6610LV) images at a magnification of 1000x were used to monitor the morphology changes during torrefaction.

Hydrophobic behaviour was studied through contact angle and wettability by liquid penetration experiments.

In contact angle test the procedure is the same as the one in [20] which is briefly explained as follows. Initially both 600 mg of torrefied as well as 600 mg of raw SRCW samples were pressed using a hydraulic press (Specac) obtaining a 13 mm diameter pellet, the pressure in the hydraulic press was 5 metric tons. Contact angles (θ) on pellet surfaces were measured using a CAM 200 optical contact angle meter (KSV Instruments Ltd.). Sessile water droplets were placed on the wood pellet surfaces and allowed to spread freely on the surface. Spreading images were captured by a high-resolution CCD camera at

40 ms intervals for 0.4 s. Contact angles were determined using the KSV CAM 200 software.

Regarding wettability by liquid penetration experiments, 1 g of powder solid is placed on a cylindrical metallic tube with porous bottom and two screw threads in order to uniformly pack the sample. Wettability measurements were made by Sigma 700 tensiometer (KSV Instruments Ltd., Helsinki, Finland). The porous bottom of the cylinder is brought into contact with water and the water rises the bottom and then through the sample. All experiments were made during 20 minutes, since first measurements made to more hydrophilic sample (raw material) shows constant mass after this point. Square mass versus time is recorded for all samples studied.

Washburn equation could be used to compare the wettability of samples measured by liquid penetration method (equation 1)

$$m^2 = \frac{C\rho^2\gamma\cos\theta}{\eta}\ t \qquad (1)$$

Where C is parameter for the packing particles arrangement and can be determined by equation 2, ρ, γ, η are the density, surface tension and the viscosity of the liquid, θ is the contact angel of the liquid on the solid and t is the time.

$$C = \frac{rA^2\varepsilon^2}{2} \qquad (2)$$

where r and A are the radius and the cross-sectional area of the packed tube respectively, and ε is the porosity of the packing tube

2.4 Gas analysis

Released gases at optimal torrefaction temperature and inert atmosphere was

characterized using pyrolysis gas chromatography/mass spectrometry (Py-GC/MS) using the same methodology as in previous work [20], which is explained in the following lines so that the reader may know it. For this test, a micro-furnace type double-shot pyrolyzer model PY2020iD (Frontier Lab Ltd.) attached to a GC/MS system (Agilent 6890) was used. 4 mg of sample was placed in a small crucible capsule and introduced in a pre-heated furnace (at optimal torrefaction temperature) in inert atmosphere. The sample was kept for 2 minutes at this temperature before the evolved gases where directly injected in the GC/MS for analysis.

The GC was used with a fused silica capillary column HP 5MS (30 m × 250 μm × 0.25 μm inner diameter), oven temperature was held at 50 °C for 1 min and then increased up to 100 °C at 30 °C min-1, from 100 to 300 °C at 10 °C min-1 and isothermal at 300 °C for 10 min using a heating rate of 20 °C min^{-1} in the scan modus. Helium was used as carrier gas with a controlled flow of 1 ml min^{-1}. The detector consisted of an Agilent 5973 mass selective detector and mass spectra were acquired with a 70 eV ionizing energy within the scan interval 50-550 m/z.

Compound assignment was achieved via single ion monitoring for different homologous series, low resolution MS and comparison with published and stored (NIST and Wiley libraries) data. Semi-quantitative calculations were performed on the pyrograms, by integrating the chromatographic peaks corresponding to identified compounds and converting the obtained areas into relative percentages. The type of the biogenic compound was also indicated.

2.5. Kinetics of torrefaction and combustion

Kinetics of torrefaction process were obtained using a thermogravimetric analyser (Perkin Elmer STA 6000) using 4 mg of the sample and carrying on torrefaction at optimal torrefaction temperature withing inert atmosphere of nitrogen with a controlled flow of 200 ml min^{-1} and the temperature program described by Chen and Kuo [7]. The isothermal single-step kinetic model was assumed for both oxidative and non-oxidative torrefaction, since the change in temperature in oxidative torrefaction is negligible due to the high flow of the carrier gas used within TGA experiments, further information about kinetic model and kinetical calculations can be found in [20].

In addition, combustion kinetics of torrefied biomass were obtained using a thermogravimetric analyser (Perkin Elmer STA 6000) following the method described by Álvarez *et al.* [37]. Since combustion is a non-isothermal process, non-isothermal kinetics are calculated and the Coats-Redfern method was assumed [38]. The whole conversion range was covered considering two stages.

3. RESULTS AND DISCUSSION

3.1. Mass and energy yields

The mass and energy yields of oxidatively and non-oxidatively torrefied biomass are depicted in Figure 1. Comparing both pretreatments, there are few differences in mass and energy yields between oxidative torrefaction and non-oxidative one, although both yields are slightly higher for oxidative torrefaction. The optimal balance of mass and energy for biomass torrefaction is 80 % of mass yield and 90 % of energy yield and since data for all the experiments were

180 higher, all the conditions would be suitable for pretreating biomass [39–41].

181 **3.2. Proximate and ultimate analysis**

182 The proximate analysis (Table 2) shows that as the torrefaction temperature
183 increases, the moisture content decreases. The drop in the moisture content
184 was more severe in oxidative torrefaction for 200 ºC and 210 ºC. In addition,
185 volatile matter decreases while fixed carbon content increased as the
186 torrefaction conditions become more severe. Ash content of torrefied SRCW is
187 slightly higher than in raw SRCW.

188 Figure 2 shows how both atomic O/C and H/C ratios decrease as the
189 torrefaction temperature rise. This is due to the removal of moisture and light
190 volatiles, which contains more hydrogen and oxygen than carbon [42], so
191 biomass is closer to fossil fuels in terms of ultimate analysis.

192 From the results of proximate and ultimate analysis, it can be concluded that
193 torrefaction of biomass leads to C-enriched biomass due to O/C and H/C ratios
194 changes together with fixed carbon content increase and this is directly related
195 to HHV increase.

196

197 Table 2. Proximate analysis of torrefied SRCW.

Sample		Moisture, %	Ash, %	Volatiles, %	Fixed Carbon, %
Non-oxidative	**200 °C**	2.5±0.6	0.9±0.2	79.3±0.3	17±2
	210 °C	1.55±0.02	0.9±0.2	77±3	20±4
	220 °C	1.30±0.08	0.9±0.3	78±4	20±5
	230 °C	1.3±0.2	0.99±0.02	71.5±0.4	26.2±0.7
	240 °C	1.2±0.4	1.28±0.07	70.5±0.5	27±1
Oxidative	**200 °C**	1.52±0.05	0.76±0.02	82±2	16±3
	210 °C	1.5±0.1	0.8±0.2	79±4	19±5
	220 °C	1.5±0.1	0.84±0.06	77.5±0.9	20±2

230 °C	1.4±0.2	0.9±0.3	75±2	23±3
240 °C	1.28±0.02	0.9±0.1	74±2	24±3

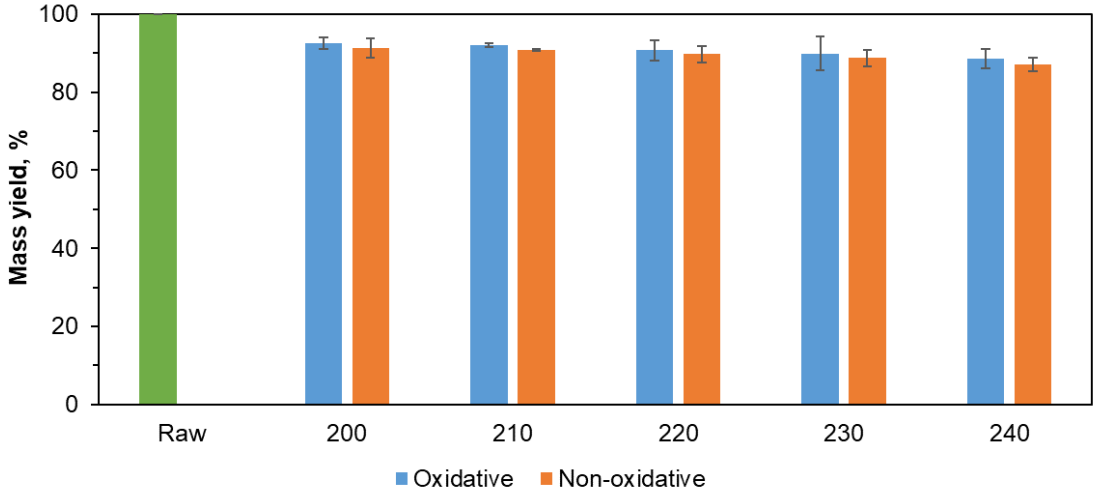

a

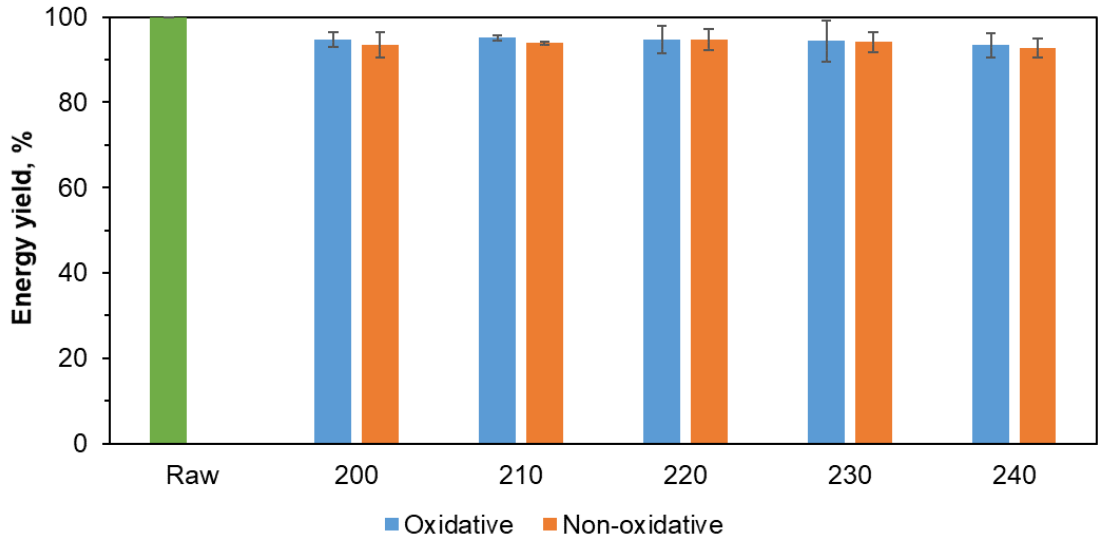

b

198 Figure 1. Mass yield (a) and energy yield (b) of SRCW obtained from oxidative

199 and non-oxidative torrefaction.

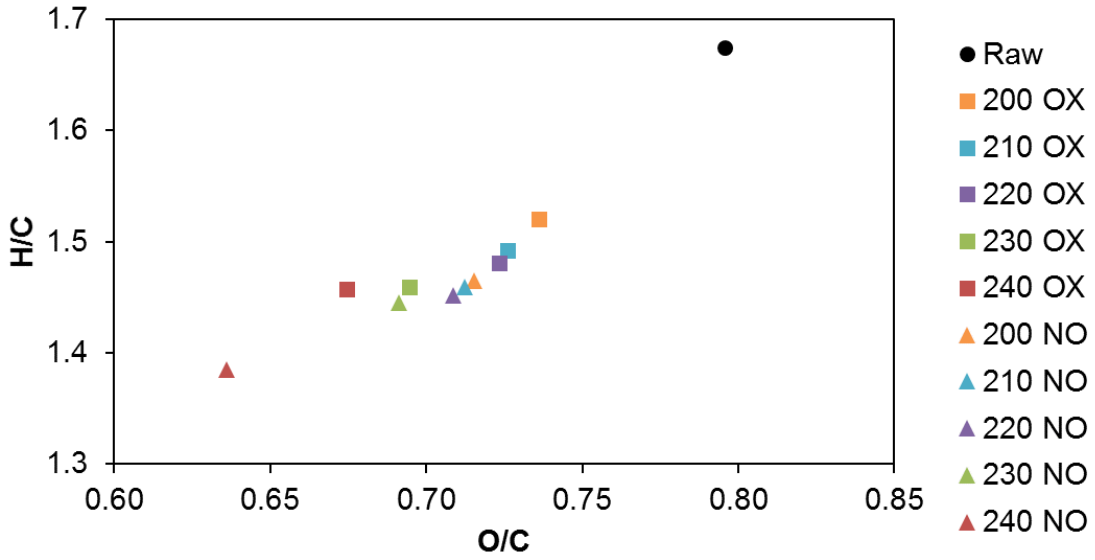

Figure 2. Van Krevelen diagram of oxidative (squares) and non-oxidative (triangles) torrefied SRCW.

3.3. Compositional analysis

Regarding compositional analysis (Table 3), lignin content increases as torrefaction conditions become more severe. Lignin content is slightly higher in non-oxidative torrefaction, this fact is explained because the lignin was more affected in oxidative torrefaction than in non-oxidative one.

Although all the literature state that hemicellulose is the most affected sample, in this case cellulose is the most affected one. This could be explained by the age of SRCW (only 4 years). For immature biomass such as SRCW, cellulose chains are not as developed as the ones in other older biomass samples such as pine, this could lead to a lower thermal degradation temperature and lower crystallinity for cellulose.

Table 3. Compositional analysis of torrefied SRCW.

Sample	Holocellulose, %	Cellulose, %	Hemicellulose, %	Lignin, %
Raw	72.7±0.5	39±2	34±3	24.2±0.8

Non-oxidative	**200°C**	74±2	34±1	40±3	25±1
	210°C	74±1	35±2	39±3	27±2
	220°C	77±4	35.1±0.5	42±5	29±4
	230°C	79±2	34±1	45±3	30.4±0.9
	240°C	75±3	29±1	46±4	32.9±0.8
Oxidative	**200°C**	81.0±0.5	41±5	40±6	27±2
	210°C	78±1	44±4	34±5	27.9±0.7
	220°C	80.4±0.2	37±4	43±5	29±2
	230°C	76±2	39±3	36±5	31±2
	240°C	77±4	31.2±0.9	46±5	31±2

3.4. Morphology changes

Some images from holocellulose from torrefied SRCW were shown in Fig. 3. Accordingly to previous results, hemicellulose is the most affected component of biomass during torrefaction and this can be observed in Fig. 3, in which small pits are seen for low torrefaction temperatures and these pits are enlarge when torrefaction conditions become more severe. The main change for oxidative torrefaction occurs at 220ºC, whereas the one for non-oxidative torrefaction takes place at 240ºC.

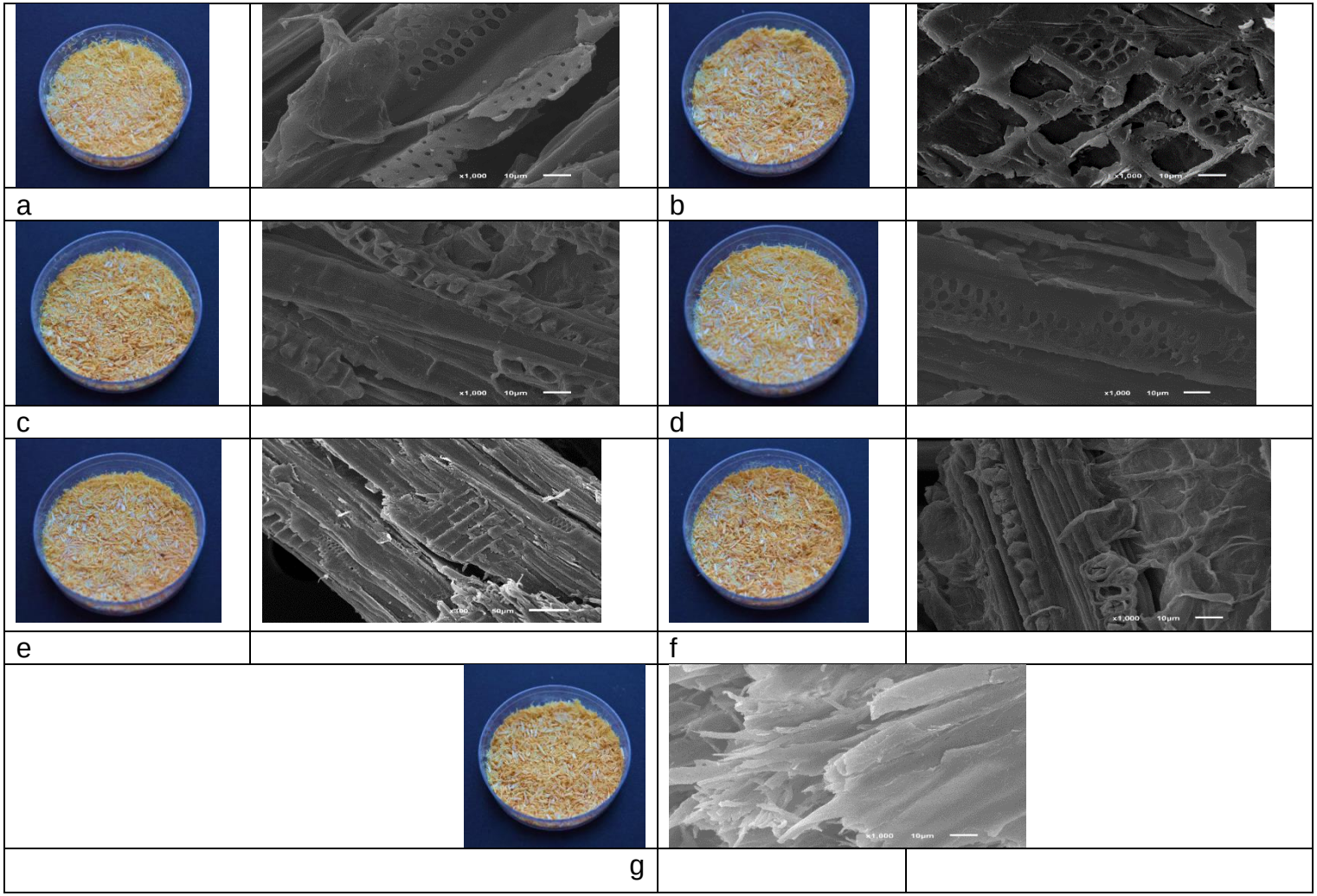

Fig. 3. SEM images from (a), (b) and (c) holocellulose obtained from oxidatively torrefied SRW at 200ºC, 220ºC and 240ºC, respectively, (d), (e) and (f) holocellulose obtained from non-oxidatively torrefied SRW at 200ºC, 220ºC and 240ºC, respectively and (g) holocellulose from raw SRCW.

3.5. Hydrophobicity measurements

The contact angle measurements showed that there was an overall trend of a positive correlation between the torrefaction temperature treatment and contact angle. Figure 4 shows the picture of the contact angles obtained. The tendency of the contact angle values recorded for different temperatures of torrefaction at oxidative and non-oxidative conditions is presented in Figure 5.

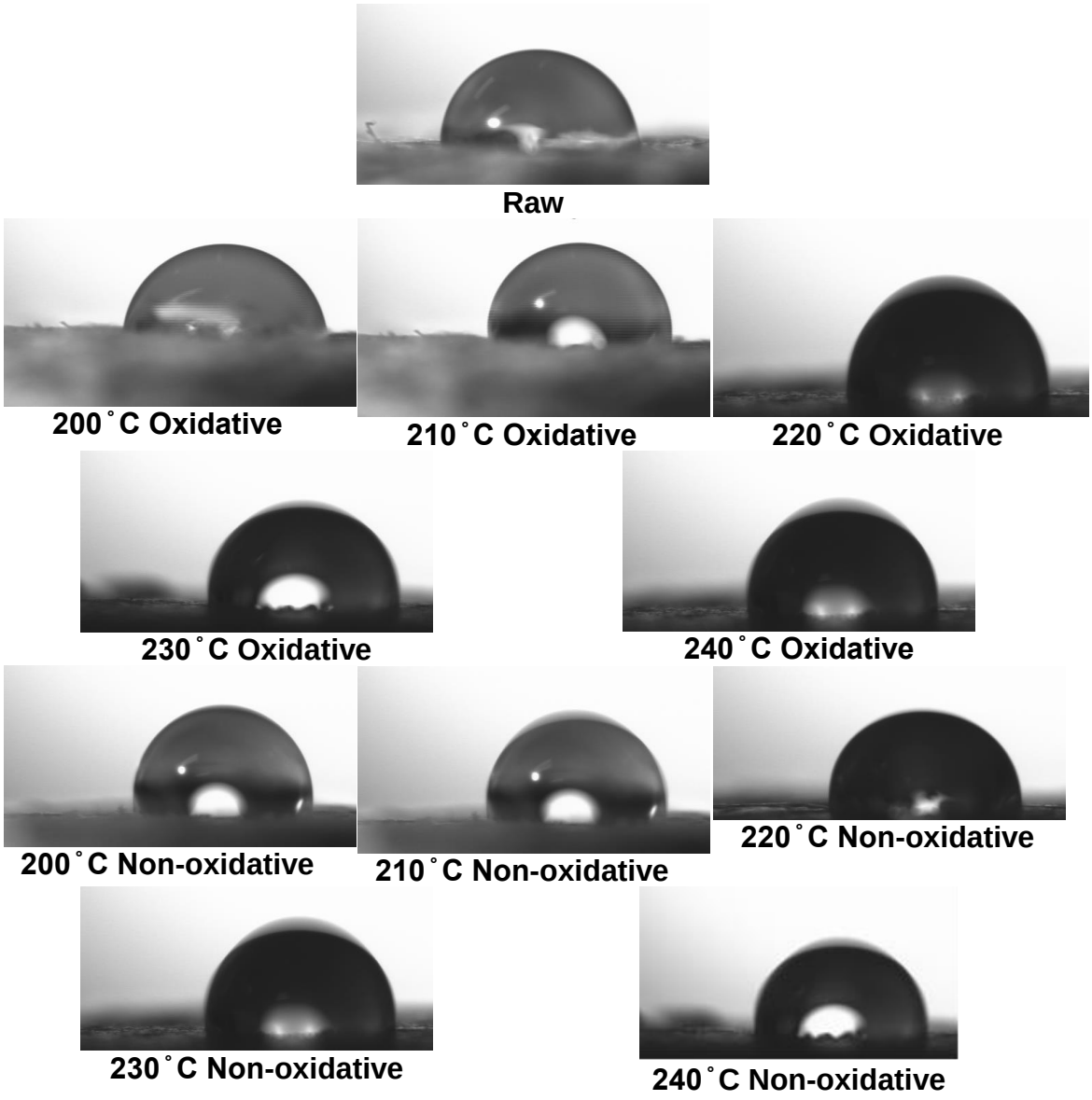

Figure 4. Pictures of the contact angles recorded with CAM 200 optical contact angle meter.

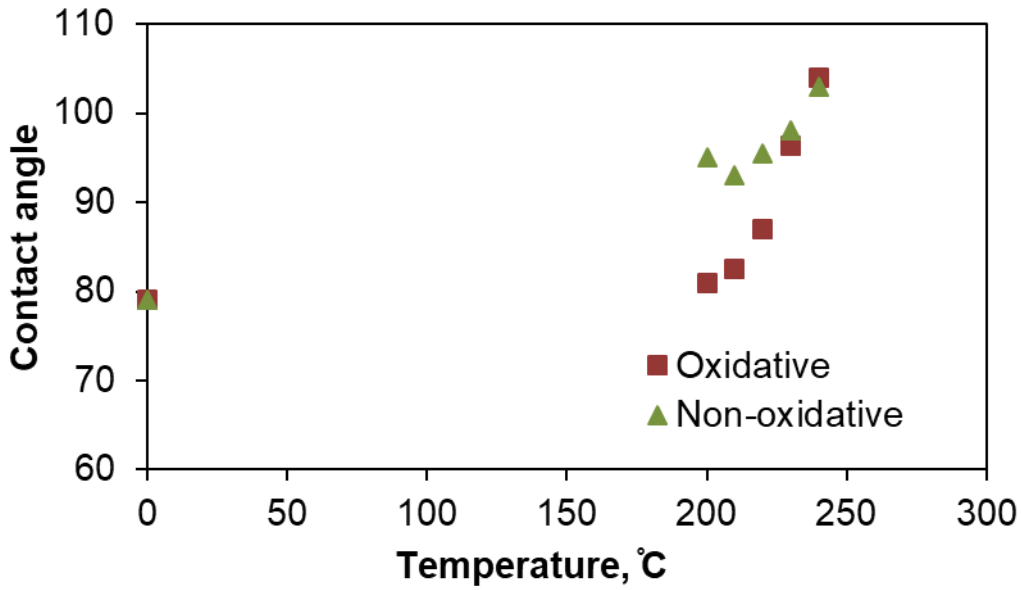

Figure 5. Contact angle versus roasted temperature for samples made by oxidative and non-oxidative process.

The values obtained ranged from 78-105° for all the samples studied. The raw samples (with no torrefaction treatment) have a value of 78.2 ± 8°and as the temperature increases the contact angle increases indicating the more hydrophobicity of the samples. Samples treated with non-oxidative process have large contact angle measurements in all cases, indicating their major effectivity respect the oxidative process in the hydrophobic treatment. In fact, for oxidative process values temperatures of 230°C are necessary in order to get high contact angle with values similar to the ones obtained with the non-oxidative treatment. Moreover, the tendency between the contact angle water-biomass and the torrefaction temperature when oxidative and non-oxidative atmospheres were used was found to have high dependence with the nature of the tested biomass.[43]

Works in which biomass was torrefied by non-oxidative atmosphere, contact

angle between biomass and water of around 80º was registered when heating treatment was carried out at 280ºC for softwood biomass species, *Abies pectinata* [44], while values around 110º were obtained for heating treatment of Indian *Acacia nilotica* [43].

Mass values versus time obtained with tensiometer instrument, when powder is in contact with deionized water, are presented in Figure 6 for oxidative and non-oxidative torrefaction treatment. Similar trend to the one obtained with the contact angle is recorded.

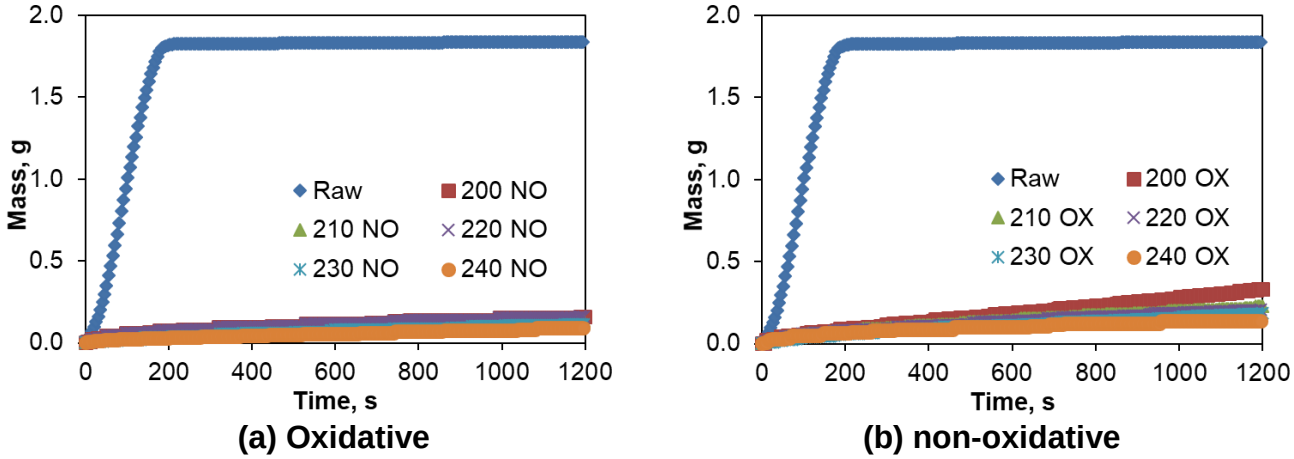

Figure 6. Mass versus time for all samples with oxidative torrefaction (a) and non-oxidative torrefaction (b)

All torrefied samples have higher hydrophobicity than the raw material, since less than half the amount of water is absorbed by the roasted sample respect the raw material. As a general trend, higher hydrophobicity is observed in the non-oxidative torrefaction treatment respect the oxidative ones, indicating higher efficiency on hydrophobicity treatment by the non-oxidative atmosphere.

In Table 4 the amount of water mass absorbed after 20 minutes of contact of

solid and water is shown.

Table 4. Mass ratio (absorbed water/biomass mass) absorbed by samples after 20 minutes on liquid penetration method

Torrefaction temperature, °C	Oxidative	Non-oxidative
	Mass, g	Mass, g
Raw	1.36	
200	0.57	0.47
210	0.46	0.42
220	0.45	0.42
230	0.37	0.40
240	0.14	0.31

The higher hydrophobicity presented by torrefied samples, especially the ones under non-oxidative atmosphere, could be related to the compositional modifications of the biomass during heating treatment as it is found in other studies where several types of biomass are torrefied at several temperatures, in these studies it was found that high temperature leads to hemicellulose degradation and, hence, the hydrophilicity of the biomass was reduced [45]. Moreover, a recent study had found higher hydrophobicity of lignin derivatives samples when lignin OH^- groups where reduced [46]. In the present study it was found a decrease of oxygen and hydrogen and an increase of carbon when torrefaction temperature increased (Figure 2) what could justify the higher hydrophobicity of the samples treated under higher temperatures, since the higher hydrophobicity of materials is normally linked to the higher concentration of carbon atoms on the molecular structure of the material.

3.6. Gas analysis

The pyrogram of the samples are depicted in Figure 7 and the family compounds were showed on Table 5. Different types of compounds were released at the optimal temperature. Polysaccharides fraction is not as high as usual since the main decomposition products of cellulose and hemicellulose are carbon dioxide, water and acetic acid which are not identified in these experiments. Lignin derivatives are the main products and it can be pointed out that no H units, which are common in herbaceous samples, were not found, additionally, the amount of S and G units are almost the same. The mixture of S and G units showed is typical in angiosperms plants as willow.

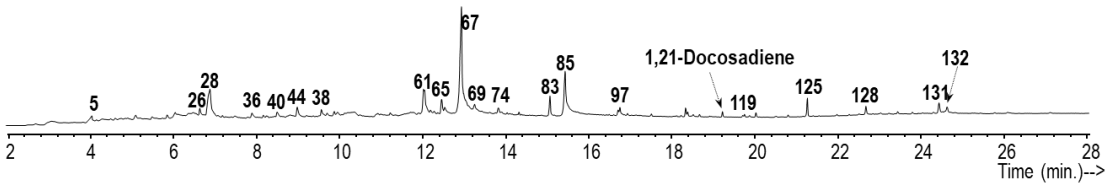

Table 5. Released gases of the samples at 240 ºC from Py-GC-MS as percentage of total chromatographic area.

Type of compound	SRCW
Aromatic	1.82
Lignin (G)	36.98
Lignin (H)	0.00
Lignin (S)	31.12
Lignin (TOTAL)	68.10
Lipid	10.75
Polysaccharides	15.18
Sterols	1.37

Figure 7. Pyrogram of SRCW. Numbers on the peaks correspond to those in The main compounds of G and S units were respectively the conipheryl aldehyde and sinapaldehyde, there are the main compounds released too (Table A.1 in supplementary content). The release of light volatiles such as

306 vanillin, vinylguaiacol or hydroxymethylfurfural is responsible for the reduction of
307 hydrogen and oxygen contents reported by the ultimate analysis in 3.1. In
308 addition, the products released during torrefaction could have different
309 applications such as the anti-inflammatory effect of conipheryl aldehyde [47]
310 and its ability to promote rapid re-proliferation of the intestinal epithelium [48] or
311 the anti-hyperglycemic and anti-obesity effects of sinapaldehyde [49].
312 The type of compounds found can be compared to another woody biomass
313 samples such as the ones in [20]. Some differences can be observed, for
314 instance, resin and terpenoids are exclusive for gymnosperms. In addition, the
315 amount of lipids in SRCW is similar to eucalyptus.

316 **3.7. Kinetics of torrefaction**

317 As the torrefaction is an isothermal process, isothermal kinetics can be
318 obtained. Theoretical part of isothermal kinetics can be found on previous work
319 [20]. The conversion of the sample is defined by equation 3:

$$\alpha = \frac{W_i - W}{W_i - W_f} \quad (3)$$

320 where W_i and W_f are the initial (105 ºC) and final (800 ºC) weights of the sample
321 respectively, while W is the weight of the sample at time t.
322 Typically, the order of reaction is not unity for torrefaction processes, thus its
323 integral kinetic equation is defined by equation 4:

$$(1-\alpha)^{1-n} - (1-\alpha_0)^{1-n} = k(n-1)(t-t_0) \quad (4)$$

324 For torrefaction of SRCW, the order of reaction found is 2 and the rate constant,
325 k, is around $4.6 \cdot 10^{-5}$ s^{-1} for non-oxidative torrefaction and $3.6 \cdot 10^{-5}$ s^{-1} for
326 oxidative one (Table 6). This rate constant is close to the value calculated on

327 the basis on the results of Chen and Kuo for hemicellulose at 240 ºC, $6 \cdot 10^{-5}$ s^{-1}
328 [7] and other mature biomass such as pine, eucalyptus, chestnut or holm oak
329 [20], so it can be concluded that torrefaction kinetic parameters do not
330 excessively change from young biomass such as SRCW to mature biomass
331 with more lignified structure, despite SRCW is slightly more reactive than those
332 biomass samples.

333 Table 6. Kinetic constant and order of reaction of the torrefaction process.

	Torrefaction temperature, ºC	k, s^{-1} (x10^5)	R^2
Oxidative	200	2.6	0.997
	210	3.1	0.996
	220	3.6	0.998
	230	6.1	0.995
	240	7.6	0.990
Non-oxidative	200	2.9	0.992
	210	1.7	0.990
	220	3.6	0.990
	230	4.4	0.991
	240	5.4	0.98

334

335 Regarding combustion kinetics of torrefied biomass, the results for Coats-
336 Redfern method are shown in Table 7. From the results, it can be stated that
337 kinetic parameters are similar to the ones in literature for other tree chips, but
338 significantly lower than those reported by López-González *et al.* [50], which
339 means that torrefied SRCW show higher reactivity than raw SRCW. Comparing
340 both samples, reactivity of oxidatively torrefied biomass is higher than non-
341 oxidatively torrefied one.

342 Table 7. Kinetic parameters of torrefied biomass combustion.

Sample	Ea 1ºStage	Ea 2ºStage	k_0 1ºStage (min^{-1})	k_0 2ºStage (min^{-1})	R^2 1ºStage	R^2 2ºStage

	(kJ/mol)	(kJ/mol)				
Oxidative	49.6	53.7	2692	2425	0.990	0.990
Non-oxidative	55.1	58.4	8662	5948	0.990	0.98

4. CONCLUSIONS

Non-oxidatively and oxidatively torrefied SRCW samples were fully characterized. The optimal torrefaction temperature turned out to be 240 ºC for the target mass and energy yields. The moisture content was reduced, and the fixed carbon was increased. The decrease of both atomic ratios H/C and O/C was demonstrated through the van Krevelen diagram, which resulted in higher values of HHV. G and S units from lignin were identified in the Py-GC/MS experiments. It was demonstrated that biomass turns hydrophobic by contact angle and liquid penetration experiments. The order of reaction obtained was 2 and the kinetic constant was around $4 \cdot 10^{-5} s^{-1}$.

AKNOWLEDGEMENTS

This article is greatly indebted to MINECO for the economic support given to the Normalized vegetable Biomass for Efficient Energetic Trigeneration project (MINECO-13-CTQ2013-45155-R) and Consejería de Economía y Empleo del Principado de Asturias for the economic support given to the TRIBIONOR project (PCTI Asturias 2013–2017, Ref. FC-15-GRUPIN14-095), which makes the continuation of research in this field possible. A. Álvarez acknowledges receipt of a graduate fellowship from the Severo Ochoa Program (Principado de Asturias, Spain).

REFERENCES

[1] Castaño-Díaz M, Álvarez-Álvarez P, Tobin B, Nieuwenhuis M, Afif-Khouri E, Cámara-Obregón A. Evaluation of the use of low-density LiDAR data to estimate structural attributes and biomass yield in a short-rotation willow coppice: an example in a field trial. Ann For Sci 2017;74:69. https://doi.org/10.1007/s13595-017-0665-7.

[2] Pereira S, Costa M. Short rotation coppice for bioenergy: From biomass characterization to establishment – A review. Renew Sustain Energy Rev 2017;74:1170–80. https://doi.org/10.1016/j.rser.2017.03.006.

[3] Cahyanti MN, Doddapaneni TRKC, Kikas T. Biomass torrefaction: An overview on process parameters, economic and environmental aspects and recent advancements. Bioresour Technol 2020;301:122737. https://doi.org/10.1016/j.biortech.2020.122737.

[4] Gent S, Twedt M, Gerometta C, Almberg E. Chapter Five - Techno-Economic Considerations of Torrefaction. Theor. Appl. Asp. Biomass Torrefaction, Butterworth-Heinemann; 2017, p. 97–121. https://doi.org/10.1016/B978-0-12-809483-9.00005-1.

[5] Collard F-X, Carrier M, Görgens JF. Chapter 4 - Fractionation of Lignocellulosic Material With Pyrolysis Processing. In: Mussatto SI, editor. Biomass Fractionation Technol. Lignocellul. Feedstock Based Biorefinery, Amsterdam: Elsevier; 2016, p. 81–101. https://doi.org/10.1016/B978-0-12-802323-5.00004-9.

[6] Chen D, Gao A, Ma Z, Fei D, Chang Y, Shen C. In-depth study of rice husk torrefaction: Characterization of solid, liquid and gaseous products, oxygen migration and energy yield. Bioresour Technol 2018;253:148–53. https://doi.org/10.1016/j.biortech.2018.01.009.

[7] Chen W-H, Kuo P-C. Isothermal torrefaction kinetics of hemicellulose, cellulose, lignin and xylan using thermogravimetric analysis. Energy 2011;36:6451–60. https://doi.org/10.1016/j.energy.2011.09.022.

[8] Chen W-H, Kuo P-C. Torrefaction and co-torrefaction characterization of hemicellulose, cellulose and lignin as well as torrefaction of some basic constituents in biomass. Energy 2011;36:803–11. https://doi.org/10.1016/j.energy.2010.12.036.

[9] Chen W-H, Kuo P-C. A study on torrefaction of various biomass materials and its impact on lignocellulosic structure simulated by a thermogravimetry. Energy 2010;35:2580–6. https://doi.org/10.1016/j.energy.2010.02.054.

[10] Acharya B, Dutta A. Fuel property enhancement of lignocellulosic and nonlignocellulosic biomass through torrefaction. Biomass Convers Biorefinery 2016;6:139–49. https://doi.org/10.1007/s13399-015-0170-x.

[11] Bridgeman TG, Jones JM, Shield I, Williams PT. Torrefaction of reed canary grass, wheat straw and willow to enhance solid fuel qualities and combustion properties. Fuel 2008;87:844–56. https://doi.org/10.1016/j.fuel.2007.05.041.

[12] Chen W-H, Cheng W-Y, Lu K-M, Huang Y-P. An evaluation on improvement of pulverized biomass property for solid fuel through torrefaction. Appl Energy 2011;88:3636–44. https://doi.org/10.1016/j.apenergy.2011.03.040.

[13] Ibrahim RHH, Darvell LI, Jones JM, Williams A. Physicochemical characterisation of torrefied biomass. J Anal Appl Pyrolysis 2013;103:21–30.

https://doi.org/10.1016/j.jaap.2012.10.004.
[14] Gao N, Li A, Quan C, Du L, Duan Y. TG–FTIR and Py–GC/MS analysis on pyrolysis and combustion of pine sawdust. J Anal Appl Pyrolysis 2013;100:26–32. https://doi.org/10.1016/j.jaap.2012.11.009.
[15] Ghalibaf M, Lehto J, Alén R. Fast pyrolysis of hot-water-extracted and delignified silver birch (Betula pendula) sawdust by Py-GC/MS. J Anal Appl Pyrolysis 2017;127:17–22. https://doi.org/10.1016/j.jaap.2017.09.008.
[16] Gu X, Ma X, Li L, Liu C, Cheng K, Li Z. Pyrolysis of poplar wood sawdust by TG-FTIR and Py–GC/MS. J Anal Appl Pyrolysis 2013;102:16–23. https://doi.org/10.1016/j.jaap.2013.04.009.
[17] Bach Q-V, Tran K-Q, Skreiberg Ø. Accelerating wet torrefaction rate and ash removal by carbon dioxide addition. Fuel Process Technol 2015;140:297–303. https://doi.org/10.1016/j.fuproc.2015.09.013.
[18] Chen D, Zheng Z, Fu K, Zeng Z, Wang J, Lu M. Torrefaction of biomass stalk and its effect on the yield and quality of pyrolysis products. Fuel 2015;159:27–32. https://doi.org/10.1016/j.fuel.2015.06.078.
[19] Chen Y, Liu B, Yang H, Yang Q, Chen H. Evolution of functional groups and pore structure during cotton and corn stalks torrefaction and its correlation with hydrophobicity. Fuel 2014;137:41–9. https://doi.org/10.1016/j.fuel.2014.07.036.
[20] Álvarez A, Nogueiro D, Pizarro C, Matos M, Bueno JL. Non-oxidative torrefaction of biomass to enhance its fuel properties. Energy 2018;158:1–8. https://doi.org/10.1016/j.energy.2018.06.009.
[21] Yuan Y, Lee TR. Contact Angle and Wetting Properties. Surf. Sci. Tech., Springer, Berlin, Heidelberg; 2013, p. 3–34. https://doi.org/10.1007/978-3-642-34243-1_1.
[22] Papp EA, Csiha C. Contact angle as function of surface roughness of different wood species. Surf Interfaces 2017;8:54–9. https://doi.org/10.1016/j.surfin.2017.04.009.
[23] Morrison ID, Ross S. Colloidal Dispersions: Suspensions, Emulsions, and Foams. Wiley; 2002.
[24] Wang C, Geramian M, Liu Q, Ivey DG, Etsell TH. Comparison of Different Methods To Determine the Surface Wettability of Fine Solids Isolated from Alberta Oil Sands. Energy Fuels 2015;29:3556–65. https://doi.org/10.1021/ef502709r.
[25] Alghunaim A, Kirdponpattara S, Newby BZ. Techniques for determining contact angle and wettability of powders 2016.
[26] Muster TH, Prestidge CA. Water adsorption kinetics and contact angles of pharmaceutical powders. J Pharm Sci 2005;94:861–72. https://doi.org/10.1002/jps.20296.
[27] Felix da Silva D, Tziouri D, Ahrné L, Bovet N, Larsen FH, Ipsen R, et al. Reconstitution behavior of cheese powders: Effects of cheese age and dairy ingredients on wettability, dispersibility and total rehydration. J Food Eng 2020;270:109763. https://doi.org/10.1016/j.jfoodeng.2019.109763.
[28] Wu S, Fitzpatrick J, Cronin K, Miao S. The effect of pH on the wetting and dissolution of milk protein isolate powder. J Food Eng 2019;240:114–9. https://doi.org/10.1016/j.jfoodeng.2018.07.022.
[29] Ge Y, Li D, Li Z. Effects of lignosulfonate structure on the surface activity and wettability to a hydrophobic powder. Bioresources 2014;9:7119–27.
[30] ASTM D1102-84(2013). Standard Test Method for Ash in Wood. West

Conshohocken, PA: ASTM International; 2013.
[31] ASTM E711-87(2004). Standard Test Method for Gross Calorific Value of Refuse-Derived Fuel by the Bomb Calorimeter (Withdrawn 2004). West Conshohocken, PA: ASTM International; 1987.
[32] ASTM E871-82(2013). Standard Test Method for Moisture Analysis of Particulate Wood Fuels. West Conshohocken, PA: ASTM International; 2013.
[33] ASTM E872-82(2013). Standard Test Method for Volatile Mater in the Analysis of Particulate Wood Fuels. West Conshohocken, PA: ASTM International; 2013.
[34] ASTM D1104 - 56(1978). Method of Test for Holocellulose in Wood (Withdrawn 1985) 1978.
[35] Sluiter A, Hames B, Ruiz R, Scarlata C, Sluiter J, Templeton D, et al. Determination of structural carbohydrates and lignin in biomass. Lab Anal Proced 2008;1617:1–16.
[36] TAPPI. TAPPI T 212 - One percent sodium hydroxide solubility of wood and pulp | Engineering360 2012.
[37] Álvarez A, Pizarro C, García R, Bueno JL, Lavín AG. Determination of kinetic parameters for biomass combustion. Bioresour Technol 2016;216:36–43. https://doi.org/10.1016/j.biortech.2016.05.039.
[38] Coats AW, Redfern JP. Kinetic Parameters from Thermogravimetric Data. Nature 1964;201:68–9. https://doi.org/10.1038/201068a0.
[39] Agarwal AK, Pandey A, Gupta AK, Aggarwal SK, Kushari A. Novel Combustion Concepts for Sustainable Energy Development. 1st ed. India: Springer; 2014.
[40] Arias B, Pevida C, Fermoso J, Plaza MG, Rubiera F, Pis JJ. Influence of torrefaction on the grindability and reactivity of woody biomass. Fuel Process Technol 2008;89:169–75. https://doi.org/10.1016/j.fuproc.2007.09.002.
[41] Wilén C, Jukola P, Järvinen T, Sipilä K, Verhoeff F, Kiel J, et al. Wood torrefaction: pilot tests and utilisation prospects. Kuopio: 2013.
[42] Chen W-H. Chapter 10 - Torrefaction. In: Negi S, Binod P, Larroche C, editors. Pretreat. Biomass, Amsterdam: Elsevier; 2015, p. 173–92.
[43] Zhang C, Wang C, Cao G, Chen W-H, Ho S-H. Comparison and characterization of property variation of microalgal biomass with non-oxidative and oxidative torrefaction. Fuel 2019;246:375–85. https://doi.org/10.1016/j.fuel.2019.02.139.
[44] Singh S, Chakraborty JP, Mondal MK. Torrefaction of woody biomass (Acacia nilotica): Investigation of fuel and flow properties to study its suitability as a good quality solid fuel. Renew Energy 2020;153:711–24. https://doi.org/10.1016/j.renene.2020.02.037.
[45] Hakkou M, Pétrissans M, Gérardin P, Zoulalian A. Investigations of the reasons for fungal durability of heat-treated beech wood. Polym Degrad Stab 2006;91:393–7. https://doi.org/10.1016/j.polymdegradstab.2005.04.042.
[46] Alwadani N, Ghavidel N, Fatehi P. Surface and interface characteristics of hydrophobic lignin derivatives in solvents and films. Colloids Surf Physicochem Eng Asp 2021;609:125656. https://doi.org/10.1016/j.colsurfa.2020.125656.
[47] Akram M, Kim K-A, Kim E-S, Shin Y-J, Noh D, Kim E, et al. Selective inhibition of JAK2/STAT1 signaling and iNOS expression mediates the anti-inflammatory effects of coniferyl aldehyde. Chem Biol Interact 2016;256:102–10. https://doi.org/10.1016/j.cbi.2016.06.029.
[48] Jeong Y-J, Jung MG, Son Y, Jang J-H, Lee Y-J, Kim S-H, et al. Coniferyl aldehyde attenuates radiation enteropathy by inhibiting cell death and promoting

endothelial cell function. PloS One 2015;10:e0128552. https://doi.org/10.1371/journal.pone.0128552.
[49] Camacho S, Michlig S, de Senarclens-Bezençon C, Meylan J, Meystre J, Pezzoli M, et al. Anti-obesity and anti-hyperglycemic effects of cinnamaldehyde via altered ghrelin secretion and functional impact on food intake and gastric emptying. Sci Rep 2015;5:7919. https://doi.org/10.1038/srep07919.
[50] López-González D, Avalos-Ramirez A, Giroir-Fendler A, Godbout S, Fernandez-Lopez M, Sanchez-Silva L, et al. Combustion kinetic study of woody and herbaceous crops by thermal analysis coupled to mass spectrometry. Energy 2015;90:1626–35. https://doi.org/10.1016/j.energy.2015.06.134.